www.czasopisma.pan.pl PAN www.journals.pan.pl
Chemical and Process Engineering 2018, 39 (1), 113–128
DOI: 10.24425/119103

VERIFICATION OF ZERO-DIMENSIONAL MODEL OF SOFC WITH INTERNAL FUEL REFORMING FOR COMPLEX HYBRID ENERGY CYCLES

Janusz Badur[1], Marcin Lemański[1,2], Tomasz Kowalczyk[1*], Paweł Ziółkowski[1], Sebastian Kornet[1]

[1] Institute of Fluid Flow Machinery, Polish Academy of Sciences, Fiszera 14 St., Gdańsk, 80-231, Poland

[2] ENERGA SA, Grunwaldzka 472 St., 80-309 Gdańsk, Poland

The article presents a zero-dimensional mathematical model of a tubular fuel cell and its verification on four experiments. Despite the fact that fuel cells are still rarely used in commercial applications, their use has become increasingly more common. Computational Flow Mechanics codes allow to predict basic parameters of a cell such as current, voltage, combustion composition, exhaust temperature, etc. Precise models are particularly important for a complex energy system, where fuel cells cooperate with gas, gas-steam cycles or ORCs and their thermodynamic parameters affect those systems. The proposed model employs extended Nernst equation to determine the fuel cell voltage and steady-state shifting reaction equilibrium to calculate the exhaust composition. Additionally, the reaction of methane reforming and the electrochemical reaction of hydrogen and oxygen have been implemented into the model. The numerical simulation results were compared with available experiment results and the differences, with the exception of the Tomlin experiment, are below 5%. It has been proven that the increase in current density lowers the electrical efficiency of SOFCs, hence fuel cells typically work at low current density, with a corresponding efficiency of 45–50% and with a low emission level (zero emissions in case of hydrogen combustion).

Keywords: fuel cell, SOFC, mathematical model, experiment, verification

1. INTRODUCTION

Literature on SOFC (Solid Oxide Fuel Cells) modelling is very extensive and this technology has rapidly developed in recent years. Currently there are several approaches to SOFC mathematical modelling, e.g. zero-dimensional (Akkaya, 2007; Aydin et al., 2016; Badur and Lemański, 2005; Bharadwaj et al., 2005; Bove et al., 2005; Campanari, 2001; Hauck et al., 2017; Lemański and Badur, 2004; Lemański and Karcz, 2008; Li and Chyu, 2005; Li and Suzuki, 2004; Magistri et al., 2004; Milewski et al., 2010), one-dimensional (Karcz, 2009), two-dimensional (Li and Chyu, 2005; Shen and Ni, 2015) and three-dimensional modelling (Al-Masri et al., 2014; Campanari and Iora, 2004; Celik et al., 2014; Choudharya et al., 2017; Karcz, 2007; Pianko-Oprych et al., 2014; Schluckner et al., 2014; Vakouftsi et al., 2011; Zhang et al., 2015). Each of those approaches is more or less complicated, and requires a different amount of computing power and provides different levels of information.

* Corresponding author, e-mail: tomasz.kowalczyk@imp.gda.pl

The zero-dimensional approach, also called CFM (Computational Flow Mechanics) models, is mainly used for system optimisation. A limited amount of the obtained data makes it possible to conduct many optimising calculations of cell thermodynamic parameters or of the entire complex system composed of many devices, like compressors, turbines, bottoming steam cycles, ORC, pumps or heat exchangers (Badur and Lemański, 2005; Blaise et al., 2015; Ziółkowski et al., 2017). The use of CFM modelling for SOFC parameter setting is presented in detail by Lazzaretto et al. (2004), while, different configurations of the most common combination, SOFC/GT (Solide Oxide Fule Cell – Gas Turbine) cycles, are carefully discussed by Chan et al. (2004) and Lemański (2007). A less known hybrid cycle like, e.g. SOFC/HCCI (Solide Oxide Fule Cell / Homogeneous Charge Compression Ignition), is considered in the work of Park et al., (2014). A proposed engine hybrid system (Park et al., 2014) was compared with a catalytic after burn solution and the SOFC/GT. The zero-dimensional models are also used for dynamic modelling of performance in time. In the work of D'Andrea et al. (2017), a system with SOFC fed with biogas was modelled in function of time to determine its thermal behaviour under changing power demand. In another work of San et al. (2010) a marine application for vessel propulsion was modelled.

The one-, two-, and three-dimensional models are generally used to establish thermal distribution in a fragment of a fuel cell, the whole cell or a stack of cells. Modelling using CFD (Computational Fluid Dynamics) codes can by simplified to establish e.g. mass or heat distribution in a specific geometry assuming constant mass or heat sources (Badur et al., 2017; Karcz et al., 2010; Lewandowski et al., 2011). This approach is employed by Celik et al. (2014) to determine stress distribution in the micro structure of anode. However, CFD codes may also be extended by equations representing chemical and electrochemical reactions. A paper by Zhang et al. (2015) concerns mass flow distribution optimisation where heat generation, the loss from the thermochemical reaction, is not a constant but a variable value depending on the current density. Extensive models developed by Karcz (2009); Schluckner et al. (2014) and Shen and Ni (2015) are proposed for cell design optimisation. Choudhary et al. (2017) present a CFD modelling of a SOFC stack cooperating with an auxiliary heat exchanger forming a CHP unit. The main aim of the calculation is a prediction of fuel utilisation factor, which leads to optimisation of the recirculation and the operation temperature. On the other hand, Al-Masri et al. (2014) propose a transient CFD model for estimating temperature distribution of a fuel cell stack under transient operating conditions.

Most quoted works offer voltage vs. current characteristics of a single tube for typical geometry manufactured by Siemens Power Generation. In the described mathematical fuel cell models, three main reactions take place in the fuel cell: the electrochemical reaction of hydrogen and oxygen, responsible for the generation of electricity, the reaction of steam reforming of methane and the reaction of water gas. It is also possible to use it for the electrochemical reaction of carbon monoxide with oxygen, but it has a negligible share in the production of electric current and is most often ignored in the literature (Akkaya, 2007; Badur and Lemański, 2005; Campanari, 2001; Karcz, 2009; San et al., 2010). The operating cell parameters are determined by the chemical equilibrium constant of the water gas, which is not a function of pressure but temperature. However, the equilibrium constant of the reforming reaction is a function of both, pressure and temperature. Some authors tried to connect these two constant equilibria and determine the chemical composition of the exhaust gas from the cell, although this is more difficult and requires solving equation systems using the Newton–Raphson method (San et al., 2010; Chan et.al., 2003). This method is used in models of Chan et.al. (2003) as well as those of Massardo and Lubelli (2000). A similar description of the model was proposed by Li and Suzuki (2004) and Li and Chyu (2005), who verified their calculation results based on the experiment. Campanari and Iora (2004) proposed in their model calculation of the chemical composition and the outlet temperature of the cell based solely on the equilibrium constant of the water gas reaction. In the discussed models, the voltage generated in the cell is determined from the Nernst equation (Akkaya, 2007; Badur and Lemański, 2005; Campanari, 2001; Karcz, 2009; Lemański and Badur, 2004; Massardo and Lubelli, 2000).

The significant advantage of SOFCs is their ability to use fuels other than hydrogen, which does not occur on Earth in a free form. That greatly influences the operational costs of fuel cells. There are articles describing more complex cells in which a SOFC cell model with internal fuel reforming is presented. In such cells, instead of hydrogen, methane-containing natural gas is used, which is subjected to steam reforming (Lazzaretto et al, 2004; Magistri et al., 2004). The performance of SOFCs powered not only by natural gas but also by syngas is discussed, e.g. in the work of Lemański and Karcz (2008), by different fuel compositions, Milewski et al. (2010a), by biogas in the work by Vakouftsi et al. (2011) and D'Andrea et al. (2017) or diesel reformate presented in the work of Schluckner et al. (2014).

An important issue of the accuracy of zero-dimensional model influence on the entire thermal cycle was raised in work of Magistri et al. (2004). For calculation and optimisation of complex systems, models should be as simple as possible. On the other hand, they must provide reliable data, otherwise not only the fuel cell parameters can be wrong but also the parameters of an entire system. Some authors considered in-house code (Badur and Lemański, 2005; Lemański and Badur, 2004; Lemański, 2007) but more common is an analysis of the commercial codes (D'Andrea et al., 2017; Hauck et al., 2017; Milewski et al., 2010a; Milewski et al., 2010b; Park et al., 2014).

This article aims at presenting fuel cell numerical model verification with data gathered from four experiments, available in the literature (Hirano et al, 1992; Li and Chyu, 2005; Li and Suzuki, 2004; Singhal, 2000). The model presented, based on a CFM code, allows to estimate the basic performance characteristics of a fuel cell, such as efficiency, power, temperature, chemical composition of exhaust gas and emission indicators.

1.1. Principle of operation

The principle of high temperature oxide fuel cell SOFC operation has been explained and discussed in many papers (Akkaya, 2007; Aydin et al., 2016; Badur and Lemański, 2005; Bharadwaj et al., 2005; Bove et al., 2005; Campanari, 2001; Campanari and Iora, 2004; Chan et al., 2003; Hauck et al., 2017; Li and Chyu, 2005; Li and Suzuki, 2004; Magistri et al., 2004). Fuel, pure hydrogen or hydrogen as an admixture with other compounds (methane, propane, methanol, carbon monoxide), is continuously fed to the anode, while the oxidant (pure oxygen or air) is delivered to the cathode. As a result of the electrochemical reaction of hydrogen-oxygen bonding, released electrons travel from the anode to the cathode through the electrical circuit. The circuit is closed by means of oxygen ions, which are transferred through a solid-oxide electrolyte. The electrolyte starts to conduct the ions in temperatures above 500°C. However, higher temperature provides higher ion conductivity, therefore commonly used operational temperature is in range of 900 – 1000°C. For this reason it is necessary to employ special materials to avoid cell elements breaking caused by thermal stresses (Lee et al., 2010; Celik et al., 2014).

There are several models describing the operation of SOFCs. They usually refer to the construction of tubular cells. These include one-, two- and three- dimensional mathematical models, more detailed than the zero-dimensional CFM models, that describe the entire device rather than its selected fragment (Badur et al., 2011; Badur et al., 2015; Lemański and Karcz, 2008). CFM models are based on integral equations of mass and energy balance, therefore they allow to determine the operating parameters of the cell (temperature, chemical composition of the exhaust gas, etc.) at the boundaries of the hypothetically accepted control casing. Because CFM models are sufficiently accurate, they are mainly applied as tools for predicting the behaviour of the object in boundaries, instead of penetrating the balance sheet around it, since changing parameters along that casing is less important. The essence of these models is to estimate the thermodynamic parameters at the inlets and outlets to / from the control casing. They are used to predict the operating parameters of combustion chambers, turbines, compressors, heat exchangers or more complex circuits of thermal power plants or power plants. The models can determine which component of the

system is damaged. However, determination of the exact cause of the failure is usually impossible. These calculations support CFD modelling, by defining the initial conditions for the problem, facilitating and accelerating long-term calculations.

As mentioned above, SOFCs can be powered by natural gas containing methane, syngas, biogas, hydrogen or other gases. If methane is used, the methane reforming process should be carried out by means of steam in an auxiliary or integrated unit.

The mathematical models presented in the literature refer to two types of fuel cells: with internal fuel reforming or non-reforming. The mathematical model of a fuel cell with reforming is more complex and requires modelling of additional elements such as the mixer and the pre-reformer. For a cell without internal reforming, modelling is based on the prediction of the parameters of a single tube fed with a mixture of hydrogen and other components (except hydrocarbons). Figure 1 shows a block diagram of a single tubular SOFC.

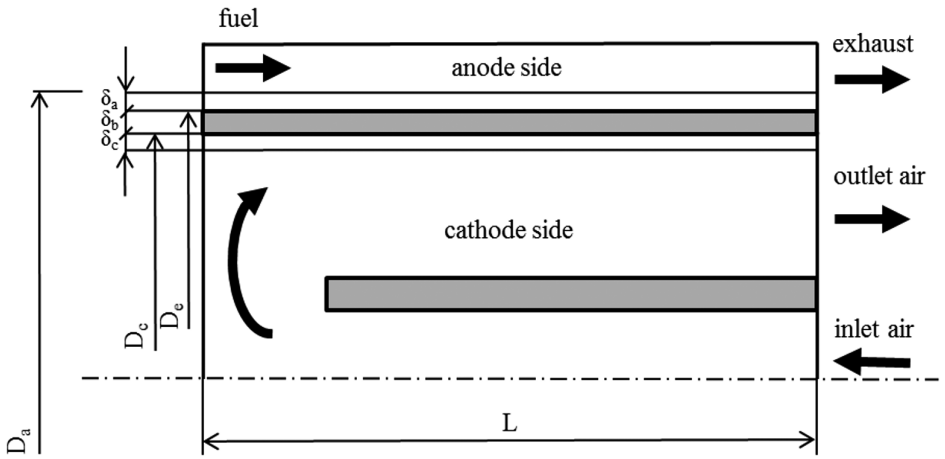

Fig. 1. Scheme of a single tube of SOFC

2. MATHEMATIC MODEL OF SOFC

Due to the paper size limitation, this work contains the most essential assumptions and simplifications adopted for the model and equations of the mathematical model of anode and cathode. All omitted data are presented in the quoted publications.

2.1. Assumptions and simplifications adopted for the model

In the presented mathematical model of a fuel cell the following assumptions and simplifications were adopted:

- the loss of heat to the environment, leaks and pressure losses were omitted;
- non-isothermal nature of the transformation and the steady state of the cell operation conditions were assumed;
- three chemical reactions in the cell: water gas reaction, reforming reaction and electrochemical reaction of hydrogen with oxygen, were modelled;
- the water gas reaction in equilibrium and the electric current generated caused only by the electrochemical reaction;

- the cell is fed by a mixture of hydrogen, carbon monoxide, carbon dioxide and water vapour, a small amount of methane is acceptable;
- air composed of argon, nitrogen and oxygen was used as an oxidant;
- the exhaust gas is a mixture of water vapour, hydrogen, oxygen, argon, nitrogen and carbon dioxide.

2.2. Mathematical model of anode and cathode

As mentioned above, in the mathematical model it is assumed that at the anode side of the fuel cell (Fig. 1), three following chemical reactions occur (Campanari, 2001):

$$\mathrm{H_2}(\dot{z}) + \frac{1}{2}\mathrm{O_2} \rightarrow \mathrm{H_2O} \tag{1}$$

where enthalpy of formation, $\Delta H_{el} = -242602$ [kJ/kmol],

$$\mathrm{CH_4}(\dot{x}) + \mathrm{H_2O} \rightarrow 3\mathrm{H_2} + \mathrm{CO} \tag{2}$$

where enthalpy of formation, $\Delta H_{ref} = 206158$ [kJ/kmol],

$$\mathrm{CO}(\dot{y}) + \mathrm{H_2O} \rightarrow \mathrm{H_2} + \mathrm{CO_2} \tag{3}$$

where enthalpy of formation, $\Delta H_{gw} = -41540$ [kJ/kmol].

As a result of the electrochemical reaction of the "cold combustion" without the flame (1), an electric current is generated in the cell I_c [A], modelled according to the following relations (Bove et al., 2005; Campanari, 2001):

$$I_c = 2 \cdot \dot{z} \cdot F \tag{4}$$

The unknown molar stream of hydrogen $\dot{z}$ [kmol/s] involved in the reaction (1), was defined on the basis of the fuel utilisation factor U_f (Bove et al., 2005; Campanari, 2001; Lemański and Badur, 2004):

$$\dot{z} = U_f \cdot \left(\dot{n}^{i,a}_{\mathrm{H_2}} + 4 \cdot \dot{n}^{i,a}_{\mathrm{CH_4}} + \dot{n}^{i,a}_{\mathrm{CO}} \right) \tag{5}$$

Introducing into Eq. (5) the fuel utilization rate U_f enables to determine the amount of fuel disposed of during the electrochemical reaction (Karcz, 2009). In a similar way, a molar stream of oxygen, $\dot{n}^{i,c}_{\mathrm{O_2}}$ [kmol/s], that is essential to initiate the reaction (1) was modelled, and was determined from the following relation (Bove et al., 2005; Campanari, 2001; Lemański and Badur, 2004):

$$\dot{n}^{i,c}_{\mathrm{O_2}} = \frac{\dot{z}}{2 \cdot U_a} \tag{6}$$

Values of fuel utilisation coefficients U_f and air utilisation coefficient U_a typically reached different levels, namely: $U_f = 80\%$ and $U_a = 20\%$, respectively (Bove et al., 2005; Campanari, 2001). This means that about 80% of hydrogen and 20% of oxygen, respectively, contained in the supplied fuel and air takes an active part in the electrochemical reaction. As a result of this process, the cell generates electrical power P_{el} [W] that is the product of current I_c [A] and voltage V_R [V]. The actual voltage of the cell V_R [V] is in fact the difference between the theoretical Nernst potential V_N [V] and the voltage loss resulting from, inter alia, loss of the resistance elements in the cell. Determination of theoretical voltage of the so-called Nernst potential V_N [V] is made according to the following relation (Campanari, 2001):

$$V_N = \frac{-\Delta G}{2 \cdot F} + \frac{R \cdot T^{o,a}}{2 \cdot F} \cdot \ln \frac{p_{\mathrm{H_2}} \cdot p^{0.5}_{\mathrm{O_2}}}{p_{\mathrm{H_2O}}} \tag{7}$$

Actual fuel cell voltage V_R [V] is reduced by activation η_{activ} [V], concentration η_{conc} [V] and resistance losses η_{ohm} [V] with respect to the Nernst potential (Lemański and Badur, 2004):

$$V_R = V_N - \eta_{activ} - \eta_{conc} - \eta_{ohm} \tag{8}$$

A detailed method of determining voltage losses and study of the effect of current exchange density i_o [A/cm^2] and the density of limited current i_l [A/cm^2] on the amount of voltage losses in the fuel cell can be found in the previous works of the authors (Badur and Lemański, 2005; Lemański, 2007; Lemański and Badur, 2004; Lemański and Karcz, 2008).

The flue gas temperature $T^{o,a}$ in Eq. (7) is the basic unknown parameter of the model under consideration. Therefore, in order to designate it, it is assumed that the reaction of water gas (3) is in thermodynamic equilibrium. Based on the equilibrium constant of the water gas reaction $K_{p,gw}$ as defined below, a desired temperature $T^{o,a}$ is determined as follows (Lemański, 2007):

$$K_{p,gw}(T^{o,a}) = \frac{\dot{n}^{o,a}_{\mathrm{H_2}} \cdot \dot{n}^{o,a}_{\mathrm{CO_2}}}{\dot{n}^{o,a}_{\mathrm{CO}} \cdot \dot{n}^{o,a}_{\mathrm{H_2O}}} \tag{9}$$

The equilibrium constant of the water gas reaction $K_{p,gw}$ is a function of temperature $T = T^{o,a}$ determined from the following polynomial function (Lemański, 2007):

$$\log K_{p,gw} = A_1 \cdot T^4 + A_2 \cdot T^3 + A_3 \cdot T^2 + A_4 \cdot T + A_5 \tag{10}$$

where the equilibrium constant coefficients assume the following values: $A_1 = 5.4700 \times 10^{-12}$, $A_2 = -2.5744 \times 10^{-8}$, $A_3 = 4.6374 \times 10^{-5}$, $A_4 = -3.9150 \times 10^{-2}$, $A_5 = 13.2097$.

The molar (or mass after inclusion molecular weight of gas component) balance of components from Eq. (9) involved in the reactions (1)–(3) was determined based on the following relations:

$$\dot{n}^{o,a}_{\mathrm{H_2}} = \dot{n}^{i,a}_{\mathrm{H_2}} + 3 \cdot \dot{x} + \dot{y} - \dot{z} \tag{11}$$

$$\dot{n}^{o,a}_{\mathrm{CH_4}} = \dot{n}^{i,a}_{\mathrm{CH_4}} - \dot{x} \tag{12}$$

$$\dot{n}^{o,a}_{\mathrm{H_2O}} = \dot{n}^{i,a}_{\mathrm{H_2O}} - \dot{x} - \dot{y} + \dot{z} \tag{13}$$

$$\dot{n}^{o,a}_{\mathrm{CO}} = \dot{n}^{i,a}_{\mathrm{CO}} + \dot{x} - \dot{y} \tag{14}$$

$$\dot{n}^{o,a}_{\mathrm{CO_2}} = \dot{n}^{i,a}_{\mathrm{CO_2}} + \dot{y} \tag{15}$$

$$\dot{n}^{o,c}_{\mathrm{O_2}} = \dot{n}^{i,c}_{\mathrm{O_2}} - 0.5 \cdot \dot{z} \tag{16}$$

$$\dot{n}^{o,c}_{\mathrm{N_2}} = \dot{n}^{i,c}_{\mathrm{N_2}} \tag{17}$$

$$\dot{n}^{o,c}_{\mathrm{Ar}} = \dot{n}^{i,c}_{\mathrm{Ar}} \tag{18}$$

For defined, in this way, molar flows of the individual components, the temperature was iteratively determined $T^{o,a}$ based on the energy balance for the whole cell:

$$\begin{aligned} \sum_{l=\mathrm{CH_4}}^{l} \dot{n}^{i,a}_l \cdot h^{i,a}_l + \sum_{m=\mathrm{Ar}}^{m} \dot{n}^{i,c}_m \cdot h^{i,c}_m - \dot{x} \cdot \Delta H_{ref} - \dot{y} \cdot \Delta H_{gw} + \dot{z} \cdot \Delta H_{el} \\ = \sum_{l=\mathrm{CH_4}}^{l} \dot{n}^{o,a}_l \cdot h^{o,a}_l + \sum_{m=Ar}^{m} \dot{n}^{o,c}_m \cdot h^{o,c}_m + P_{el} \end{aligned} \tag{19}$$

where l and m change accordingly to denote CH_4, H_2, H_2O, CO, CO_2 and Ar, N_2, O_2, and h_m means the molar enthalpy of a given component in $\dot{m}^{i,a}$ [kJ/kmol].

Additionally, it is assumed, based on the numerical simulation of CFD, that the temperature at the cathode outlet $T^{o,k}$ was lower than the temperature $T^{o,a}$ by $\Delta T = 30$ K (Campanari and Iora, 2004; Karcz, 2007; Karcz, 2009).

The electrical efficiency of a fuel cell is defined as (Feidt, 2017; Sieniutycz and Jeżowski, 2009):

$$\eta_{el} = \frac{P_{el}}{\dot{m}^{i,a} \cdot LHV} = \frac{I_c \cdot V_R}{\dot{m}^{i,a} \cdot LHV} \tag{20}$$

where the mass rate of fuel supplied to the anode $\dot{m}^{i,a}$ [kg/s] was determined as:

$$\dot{m}^{i,a} = \dot{m}^{i,a}_{H_2} + \dot{m}^{i,a}_{CH_4} + \dot{m}^{i,a}_{CO} + \dot{m}^{i,a}_{CO_2} + \dot{m}^{i,a}_{H_2O} \tag{21}$$

In addition, the current density is defined i_c [A/cm^2] as a quotient of the current I_c and the active surface of the cell A_c.

3. RESULTS AND DISCUSSION

The results of the calculations were primarily verified making use of four experiments in the *3.1. Verification of the mathematic model* subsection and *3.2. Prediction of voltage and electrical power of the cell* subsection. Next the model is used for optimisation of efficiency-current and temperature-current in the *3.3. Electrical efficiency of the cell and temperature of the exhaust* subsection.

3.1. Verification of the mathematic model

The mathematical model of the cell was tested and the obtained results were compared to four available

Table 1. Fuel and oxidant parameters taken from selected experiments

Source			Hagiwara (Li and Suzuki, 2004)	Hirano (Hirano et al., 1992)	Tomlins (Li and Chyu, 2005)	Singhal (Singhal, 2000)
Parameter		Unit	Value			
Fuel volumetric composition	H_2	%	98.64	55.70	98.64	89.00
	H_2O	%	1.36	27.70	1.36	11.00
	CH_4	%	–	–	–	–
	CO	%	–	10.80	–	–
	CO_2	%	–	5.80	–	–
Fuel utilisation coefficient	U_f	–	0.85	0.80	0.85	0.85
Fuel Temperature	T	K	1173	1073	1073	1073
Oxidant volumetric composition	O_2	%	21.00	21.00	21.00	21.00
	N_2	%	79.00	79.00	79.00	79.00
Oxidant utilisation coefficient	U_a	–	0.17	0.25	0.17	0.25
Oxidant temperature	T	K	873	873	873	873

Table 2. Fuel cell tube parameters taken from selected experiments

Source			Hagiwara (Li and Suzuki, 2004)	Hirano (Hirano et al., 1992)	Tomlins (Li and Chyu, 2005)	Singhal (Singhal, 2000)
Parameter		Unit	Value			
Anode diameter	D_a	mm	16.00	21.68	22.00	22.00
Electrolyte diameter	D_e	mm	15.80	21.48	21.80	21.80
Cathode diameter	D_c	mm	15.72	21.40	21.72	21.72
Anode thickness	δ_a	mm	0.10	0.10	0.10	0.10
Electrolyte thickness	δ_e	mm	0.04	0.04	0.04	0.04
Cathode thickness	δ_c	mm	2.20	0.70	2.20	2.20
Anode specific-area resistance	ρ_a	Ω/cm^2	$0.002980 \cdot e^{\frac{-1392}{T}}$			
Electrolyte specific-area resistance	ρ_e	Ω/cm^2	$0.002940 \cdot e^{\frac{10350}{T}}$			
Cathode specific-area resistance	ρ_c	Ω/cm^2	$0.008114 \cdot e^{\frac{600}{T}}$			

experiments for a single cylindrical tube. Experimental data and parameters of fuel and oxidiser volumetric compositions are presented in Table 1, while the tube geometry and the specific-area resistance are presented in Table 2.

For all calculations the limiting current density values were assumed at $i_o = 0.67$ A/cm^2 and the exchange current density at $i_l = 0.20$ A/cm^2, respectively. However, this assumption imposes differences between the calculated values and the experimental results.

3.2. Prediction of voltage and electrical power of the cell

Typical voltage characteristics of fuel cells – current density and electrical power – current density for available experimental data are shown in the following Figs 2–6.

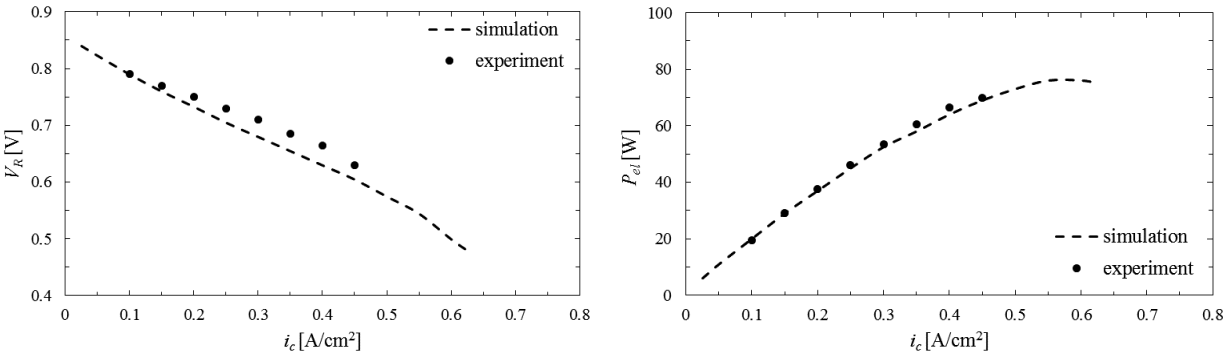

Fig. 2. Voltage-current density relation (on the left) and power-current density (on the right) – comparison of calculation results with Hagiwara experiment

The results of the Hagiwara experiment taken from the literature (Li and Suzuki, 2004), refer to the range of current density i_c from 0.10 to 0.45 A/cm^2. Numerical simulation was performed for a slightly larger

range, i_c from 0.01 to 0.62 A/cm^2. The characteristic feature of fuel cells is that the maximum electrical power reaches its peak for the high current density, as shown in Fig. 2. The greatest differences between Hagiwara's experiments and calculations do not exceed 2%.

In the next step the results of the calculations were compared to the Hirano experiments presented in the literature (Hirano et al., 1992). There are only two measurement points available, hence the comparison of both characteristics is not complete. However, the results of the calculations are qualitatively consistent with the experimental data. The difference in these results amounts to about 5%, as shown in Fig. 3.

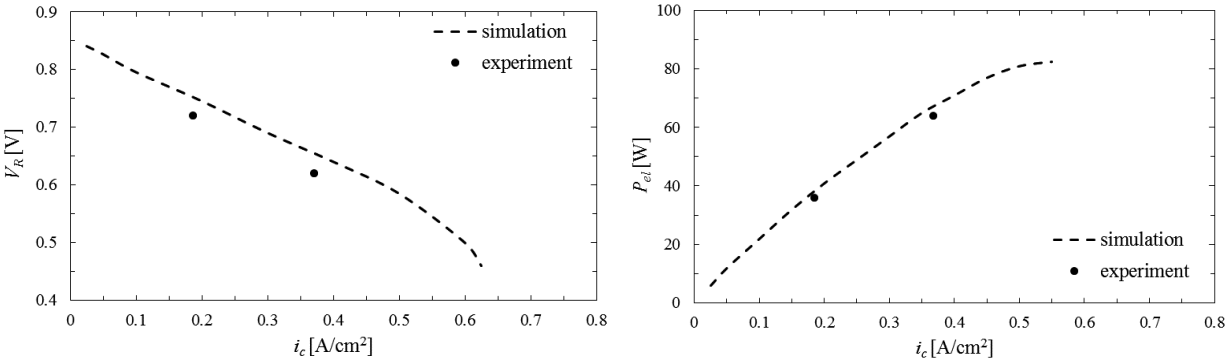

Fig. 3. Voltage-current density relation (on the left) and power-current density (on the right) – comparison of calculation results with Hirano experiment

Tomlins experiment (Li and Chyu, 2005) was the third set of experimental data of which the calculations were compared to. Fig. 4 shows the voltage and power characteristics for this cell. Significant differences in results for both the voltage and electrical power of the analysed cylindrical cell are evident. The voltage, designated by this model, is lower (up to 20%) than the experimental value. Probably the reason for this is an improperly adopted value for the limited current i_l, which depends on the angle of inclination of the voltage curve.

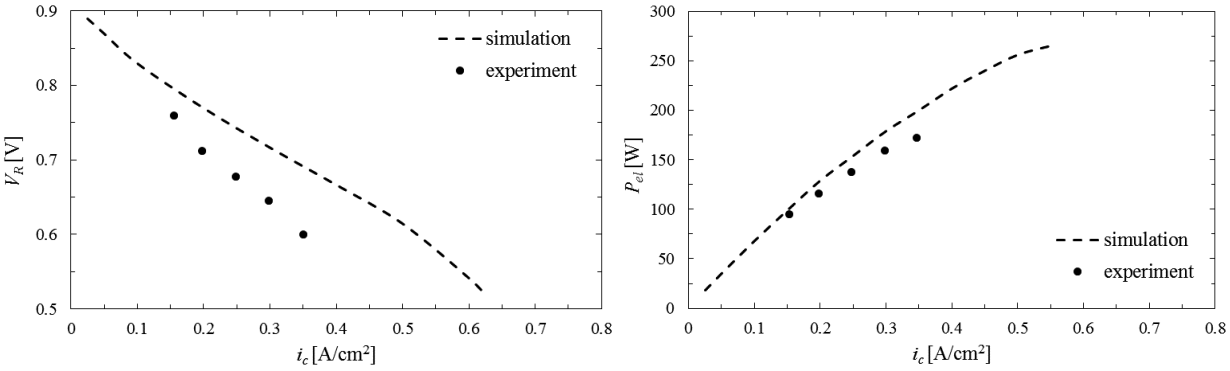

Fig. 4. Voltage-current density relation (on the left) and power-current density (on the right) – comparison of calculation results with Tomlins experiment

Diagrams in Fig. 5 present the results of the fuel cell computation and their comparison with the Singhal experimental data (Singhal, 2000). Consistency of the results is qualitatively and quantitatively satisfactory as the error is about 2%.

From the presented calculations and comparison with the experiments of Hagiwara (Li and Suzuki, 2004), Hirano (Hirano et al., 1992), Tomlins (Li and Chyu, 2005) and Singhal (Singhal, 2000), the proposed and implemented SOFC model accurately reflects the actual chemical, electrochemical and thermodynamic

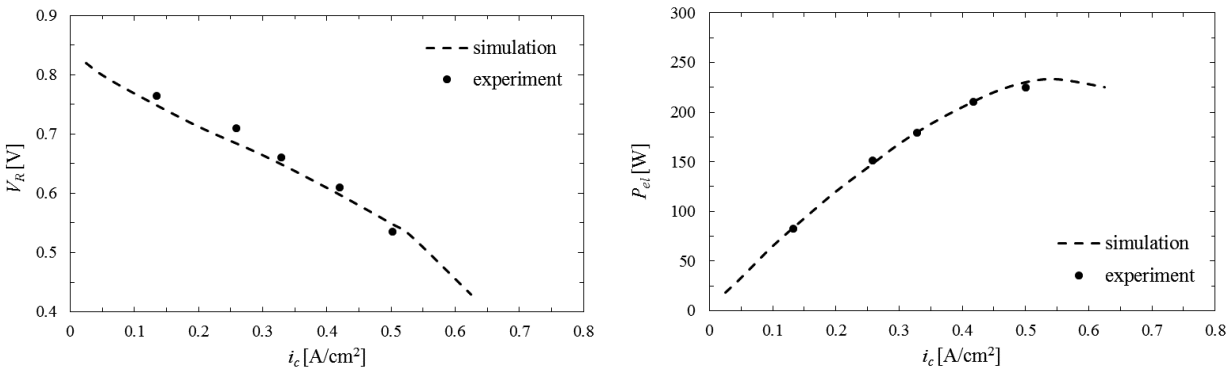

Fig. 5. Voltage-current density relation (on the left) and power-current density (on the right) – comparison of calculation results with Singhal experiment

processes occurring in the complex fuel cell. The best convergence with the experiments of Hagiwara and Singhal is obtained. However, in all analysed cases the voltage-current density and power-current density curves attain a similar shape, which proves good quality of the calculated data. An increase of the current density decreases the cell voltage and increases electric power, up to the maximum power. In should be noted that although all the tested cells have a similar voltage-current density range, the output power is different. For the Hagiwara and Hirano experiment the maximum power (from the calculations) is about 80 W, while cells tested by Tomlins and Singhal reach about 230 W and over 250 W, respectively .

3.3. Electrical efficiency of the cell and temperature of the exhaust

The presented characteristics show that for an optimum current density i_c the cell generates maximum electrical power P_{el}. From the investment standpoint, the logical solution is to design fuel cells that would work at the maximum power and a high current density. However, it would result in a decrease of electric potential V_R and in a lower cell electrical efficiency η_{el}, as is evident in Fig. 6.

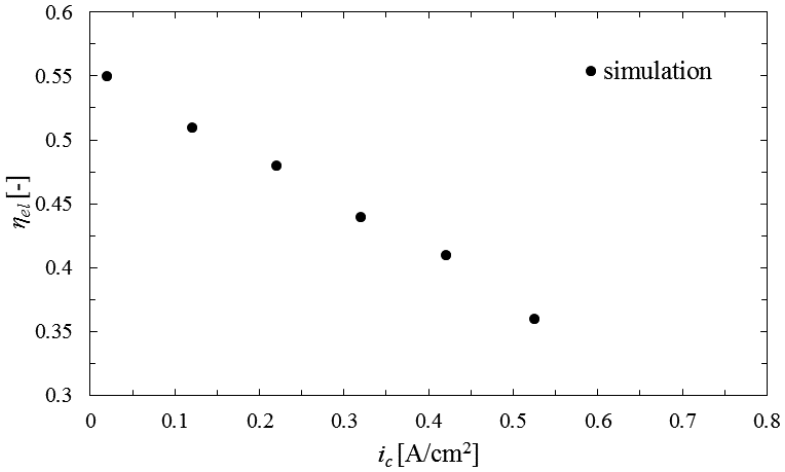

Fig. 6. Electrical efficiency-current density characteristics – calculations for the Singhal experiment

Furthermore, cells working at their maximum power could cause instable operation, because they will tend to oscillate between the current densities larger and smaller than that those at which the maximum power is achieved. In practice, cells work at compromising current densities, located on the left of the

maximum power point. This compromise between the lower cost of operation with high efficiency (low current density), and a low investment cost associated with the lower active cell area (high current density) has to be fitted. Fuel cells with a geometry corresponding to the Singhal experiment typically operate at a current density of about $i_c = 0.18$ A/cm^2 (Campanari and Iora, 2004). By analysing the characteristics shown in Fig. 6, it could be concluded that this corresponds to an electrical efficiency of about 50%. It should also be emphasised that in the case of hydrogen combustion, as in this experiment, the fuel cell is characterised by zero carbon dioxide emissions (vol.: 86.6% H_2O, 13.4% H_2).

The overall efficiency of the cell decreases due to increase of the anode side $T^{o,a}$ outlet temperature caused by the increase of the current density (Fig. 7).

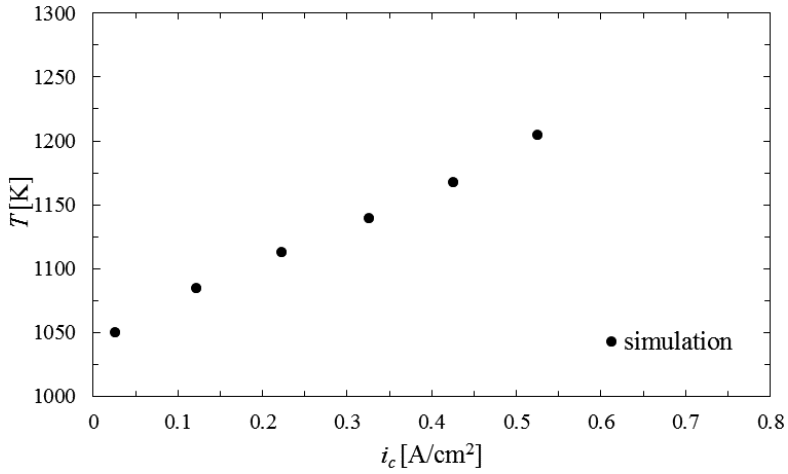

Fig. 7. Temperature at the outlet of the anode-current density characteristic – calculations for the Singhal experiment

Although high temperature of the exhaust causes thermodynamic losses, the SOFC exhaust temperature is so high that it can effectively be utilised in heat engines. Possibility of adjusting exhaust temperature in hybrid systems provides an optimisation tool for maximisation of the system efficiency in both, nominal and off-design conditions. For example, the electrical efficiency of SOFC/GT units can reach 60% and electrical power of 1.00 MWe can easily be achieved (Singhal, 2000; Singhal and Kendall, 2004).

4. CONCLUSIONS

The paper presents the characteristics of a tubular SOFC powered by methane. These characteristics were obtained using a CFM code implemented into the proprietary COM-GAS computing code. The results of calculations were compared with the available experimental data. The proposed model in qualitative and quantitative terms well reflects the complex chemical and electrochemical processes taking place in the cell. The differences between the results and experimental data do not exceed 5%. Both electric power and fuel cell efficiency were determined. As shown, fuel cells have a high energy conversion efficiency of about 50% and zero emission in the case of hydrogen as a fuel. Electrical efficiency can further be enhanced by the use of SOFC with a gas turbine in high pressure hybrid SOFC/GT system (up to 60%). It should be emphasised that in the case of currently used electricity generation technologies, their electrical efficiency varies from 40% to 45%.

Furthermore, lower emission values correspond to electricity produced by gas and steam turbines in combined cycles, for which carbon dioxide emissions are about 0.50–0.60 kg CO_2/kWh for natural gas com-

bustion (Ziółkowski et al., 2012). Higher impact on environment is achieved in supercritical steam plants, where carbon dioxide emissions are much higher and amount to about 0.80–1.10 kg CO_2/kWh for coal combustion (Ziółkowski et al., 2017). Nowadays, for methane, the emission level of SOFC with internal reforming is about 0.30 kg CO_2/kWh (Lemański, 2007), although hydrogen can be more prospective. Since hydrogen does not occur in a free form in the environment, a potential development is the use of methane in steam reforming cells. The carbon dioxide emissions of this type of fuel cell are about twice lower than those of combustion in a conventional gas burner. Therefore, from the thermodynamic and ecological points of view, SOFCs are a forward-looking technology, which can replace gas burners. On the other hand, high economic costs and low power of the systems offered as well as numerous operational problems restrict their use only to distributed power supplying sources to offices, hospitals, etc. up to 1 MWe.

Also the advantages of the developed mathematical CFM model should be emphasised. On the one hand, equations applied in these models are expressed by parameters that are relatively easy to determine in the experiment. This allows to calibrate or verify the model constants. On the other hand, the model is built in such a way that it can be implemented into general code calculating heat cycles, since the cell can cooperate with gas turbines or other devices. Another advantage of the model is its compatibility with CFD numerical codes, which allows to compute model constant values through integration over three-dimensions in local scale. To keep up with the rapidly developing nano-materials for anodes, cathodes and electrolytes, it is important to equip three-dimensional models with tools for increased mass transport mechanisms. The basics of balance equations in such materials are discussed in the papers (Badur et al., 2011; Badur et al., 2013; Badur et al., 2015; Ziółkowski and Badur, 2014), therefore we hope the development of CFM models will take into account these characteristics of nanotechnology.

The future work should focus on the dynamic load change of the power grid forced by renewable energy sources, such as wind and solar generation (Hyrzyński et al., 2013). Though the SOFCs can be dynamically loaded to meet power demand, they can also work in power to fuel mode. In this area hydrogen is looking forward to be replaced by fuels which can be easily liquefied, such as ammonia. Other possibility is synergy of electrolysis and carbon or carbon dioxide to produce methanol. The great advantage of SOFC is diversity of fuel kinds which can be used for direct supply of the cells (Rokni, 2017).

SYMBOLS

A_c	surface of the cell, m^2
CFD	Computational Fluid Dynamics (based on 3D models)
CFM	Computational Flow Mechanics (based on 0D models)
D	diameter, mm
F	Faraday's constant, C/mol
h	molar enthalpy, kJ/kmol
i_c	cell current density, A/cm^2
I_c	cell current, A
K	chemical reaction equilibrium constant
L	characteristic length of tubular cell, m
LHV	lower calorific value, kJ/kg
$\dot{m}^{i,a}$	mass rate of fuel supplied to the anode, kg/s
$\dot{n}$	molar flow of component, kmol/s
p	partial pressure, Pa
P_{el}	electrical power, W

R	universal gas constant, kJ/mol K
SOFC	Solide Oxide Fuel Cell
T	temperature, K
U_a	oxidiser utilisation coefficient
U_f	fuel utilisation coefficient
V_R	cell voltage, V
$\dot{x}$	molar stream of methane from reforming reaction, kmol/s
$\dot{y}$	molar stream of CO from shifting reaction, kmol/s
$\dot{z}$	molar stream of hydrogen from electrochemical reaction, kmol/s
ΔG	free enthalpy for electrochemical reaction, kJ/mol
ΔH	enthalpy of formation, kJ/kmol
δ	thickness, mm
η_{ohm}	losses of resistance, V
η_{conc}	losses of concentration, V
η_{activ}	losses of activation, V
η_{el}	electrical efficiency
ρ	specific-area resistance, Ω/cm^2

Subscripts

a	anode, air
c	cathode, cell
e	electrolyte
el	electrical, electrochemical
f	fuel
p, gw	gas water reaction
l, m	components of mixture in denote CH_4, H_2, H_2O, CO, CO_2 and Ar, N_2, O_2, respectively
ref	reforming reaction

Superscripts

a	anode
c	cathode
i	inlet
o	outlet

REFERENCES

Akkaya A.V., 2007. Electrochemical model for performance analysis of a tubular SOFC. *Int. J. Energy Res.*, 31, 79–98. DOI: 10.1002/er.1238.

Al-Masri A., Peksen M., Blum L., Stolten D., 2014. A 3D CFD model for predicting the temperature distribution in a full scale APU SOFC short stack under transient operating conditions. *Appl. Energy*, 135, 539–547. DOI: 10.1016/j.apenergy.2014.08.052.

Aydın O., Nakajima H., Kitahara T., 2016. Reliability of the numerical SOFC models for estimating the spatial current and temperature variations. *Int. J. Hydrogen Energy*, 41, 15311–15324. DOI: 10.1016/j.ijhydene.2016.06.194.

Badur J., Lemański M., 2005. Solid Oxide Fuel Cell (SOFC) with an internal reforming. *Chem. Process Eng.*, 26, 157–172 (in Polish).

Badur J., Karcz M., Lemański M., 2011. On the mass and momentum transport in the Navier–Stokes slip layer. *Microfluid. Nanofluid.*, 11, 439 – 449. DOI: 10.1007/s10404-011-0809-2.

Badur J., Ziółkowski P., Zakrzewski W., Sławiński D., Banaszkiewicz M., Kaczmarczyk O., Kornet S., Ziółkowski P.J., 2013. On the surface vis impressa caused by a fluid-solid contact. In: Pietraszkiewicz W., Górski J. (Eds.), *Shell Structures: Theory and Applications*. Volume 3. CRC Press, London, 53–56. DOI: 10.1201/b15684-11.

Badur J., Ziółkowski P.J. Ziółkowski P., 2015. On the angular velocity slip in nano flows. *Microfluid. Nanofluid.*, 19, 191–198. DOI: 10.1007/s10404-015-1564-6.

Badur J., Ziółkowski P., Kornet S., Stajnke M., Bryk M., Banaś K., Ziółkowski P.J., 2017. The effort of the steam turbine caused by a flood wave load. *AIP Conf. Proc.*, 1822, 020001. DOI: 10.1063/1.4977675.

Bharadwaj A., Archer D.H., Rubin E.S., 2005. Modeling the performance of a tubular solid oxide fuel cell. *J. Fuel Cell Sci. Technol.*, 2, 38–44. DOI: 10.1115/1.1842781.

Blaise M., Feidt M., Maillet D., 2015. Optimization of the changing phase fluid in a Carnot type engine for the recovery of a given waste heat source. *Entropy*, 17, 5503-5521. DOI: 10.3390/e17085503.

Bove R., Lunghi P., Sammes N.M., 2005. SOFC mathematic model for systems simulations. Part one: from a micro-detailed to macro-black-box model. *Int. J. Hydrogen Energy*, 30, 181–187. DOI: 10.1016/j.ijhydene.2004.04.008.

Campanari S., 2001. Thermodynamic model and parametric analysis of a tubular SOFC module. *J. Power Sources*, 92, 26-34. DOI: 10.1016/S0378-7753(00)00494-8.

Campanari S., Iora P., 2004. Definition and sensitivity analysis of a finite volume SOFC model for a tubular cell geometry. *J. Power Sources*, 132, 113–126. DOI: 10.1016/j.jpowsour.2004.01.043.

Celik S., Ibrahimoglu B., Toros S., Mat M.D., 2014. Three dimensional stress analysis of solid oxide fuel cell anode micro structure. *Int. J. Hydrogen Energy*, 39, 19119–19131. DOI: 10.1016/j.ijhydene.2014.09.110.

Chan S.H., Ho H.K., Tian Y., 2003. Multi–level modeling of SOFC-gas turbine hybrid system. *Int. J. Hydrogen Energy*, 28, 889–900. DOI: 10.1016/S0360-3199(02)00160-X.

Choudharya T., Sahub M., Sanjayc, 2017. CFD Modeling of SOFC cogeneration system for building application. *Energy Procedia*, 109, 361–368. DOI: 10.1016/j.egypro.2017.03.087.

D'Andrea G., Gandiglio M., Lanzini A., Santarelli M., 2017. Dynamic model with experimental validation of a biogas-fed SOFC plant. *Energy Convers. Manage.*, 135, 21–34. DOI: 10.1016/j.enconman.2016.12.063.

Feidt M., 2017. *Finite physical dimensions optimal thermodynamics 1. Fundamentals*. ISTE Press /Elsevier, London.

Hauck M., Herrmann S., Spliethoff H., 2017. Simulation of a reversible SOFC with Aspen Plus. *Int. J. Hydrogen Energy*, 42, 10329–10340. DOI: 10.1016/j.ijhydene.2017.01.189.

Hirano A., Suzuki M., Ipponmatsu M., 1992. Evaluation of a new Solid Oxide Fuel Cell system by nonisothermal modeling. *J. Electrochem. Soc.*, 139, 2744–2751. DOI: 10.1149/1.2068973.

Hyrzyński R., Karcz M., Lemański M., Lewandowski K., Nojek S., 2013. Complementarity of wind and photovoltaic power generation in conditions similar to Polish. *Acta Energetica*, 4, 14–21. DOI: 10.12736/issn.2300-3022.2013402.

Karcz M., 2007. Performance of tubular fuel cell with an internal methane reforming. *Chem. Process Eng.*, 28, 307–321.

Karcz M., 2009. From 0D to 1D modeling of tubular Solid Oxide Fuel Cell. *Energy Convers. Manage.*, 50, 2307–2315. DOI:10.1016/j.enconman.2009.05.007.

Karcz M., Kowalczyk S., Badur J., 2010. On the influence of geometric microstructural properties of porous materials on the modeling of a tubular fuel cell. *Chem. Process Eng.*, 31, 489–503.

Lazzaretto A., Toffolo A., Zanon F., 2004. Parameter setting for a tubular SOFC simulation model. *J. Energy Res. Technol.*, 126, 40–46. DOI: 10.1115/1.1653752.

Lee J.-J., Moon H., Park H.-G., Yoon D.I., Hyun S.-H., 2010. Applications of nano-composite materials for improving the performance of anode-supported electrolytes of SOFCs. *Int. J. Hydrogen Energy*, 35, 738–744. DOI: 10.1016/j.ijhydene.2009.10.089.

Lemański M., 2007. *Analysis of power cycles with fuel cell and gas-steam turbine*. PhD Dissertation IFFM PAS, Gdańsk (in Polish).

Lemański M., Badur J., 2004. Parametrical analysis of a tubular pressurized SOFC. *Archives of thermodynamics*, 25,(1), 53–72.

Lemański M., Karcz M., 2008. Performance of lignite-syngas operated tubular Solid Oxide Fuel Cell. *Chem. Process Eng.*, 29, 233–248.

Lewandowski T., Ochrymiuk T., Czerwińska J., 2011. Modeling of heat transfer in microchannel gas flow. *J. Heat Transfer*, 133, 022401–1. DOI: 10.1115/1.4002438.

Li P.W., Chyu M.K., 2005. Electrochemical and transport phenomena in solid oxide fuel cells. *J. Heat Transfer*, 127, 1344–1362. DOI: 10.1115/1.2098828.

Li P.W., Suzuki K., 2004. Numerical modeling and performance study of a tubular SOFC. *J. Electrochem. Soc.*, 151, (4), 548–557. DOI: 10.1149/1.1647569.

Magistri L., Bozzo R., Costamagna P., Massardo A.F., 2004. Simplified versus detailed solid oxide fuel cell reactor models and influence on the simulation of the design point performance of hybrid systems. *J. Eng. Gas Turbines Power*, 126, 516–523. DOI: 10.1115/1.1719029.

Massardo A.F., Lubelli F., 2000. Internal reforming Solid Oxide Fuel Cell – gas turbine combined cycles IRSOFC-GT. Part A: Cell model and cycle thermodynamic analysis. *J. Eng. Gas Turbines Power*, 122, 27–35. DOI: 10.1115/1.483187.

Milewski J., Badyda K., Miller A., 2010. Modelling the influence of fuel composition on Solid Oxide Fuel Cell by using the advanced mathematical model. *Rynek Energii*, 88, 159–163.

Milewski J., Świercz T., Badyda K., Miller A., Dmowski A., Biczel A., 2010. The control strategy for a molten carbonate fuel cell hybrid system. *Int. J. Hydrogen Energy*, 35, 2997–3000. DOI: 10.1016/j.ijhydene.2009.06.040.

Park S.H., Lee Y.D., Ahn K.Y., 2014. Performance analysis of an SOFC/HCCI engine hybrid system: System simulation and thermo-economic comparison. *Int. J. Hydrogen Energy*, 39, 1799–1810. DOI: 10.1016/j.ijhydene. 2013.10.171.

Pianko-Oprych P., Kasilova E., Jaworski Z., 2014. CFD analysis of heat transfer in a microtubular solid oxide fuel cell stack. *Chem. Process Eng.*, 35, 293–304. DOI: 10.2478/cpe-2014-0022.

Rokni M., 2017. Addressing fuel recycling in solid oxide fuel cell systems fed by alternative fuels. *Energy*, 137, 1013–1025. DOI: 10.1016/j.energy.2017.03.082.

San B., Zhou P., Clealand D., 2010. Dynamic modeling of tubular SOFC for marine power system. *J. Mar. Sci. Appl.*, 9, 231–240. DOI: 10.1007/s11804-010-1001-x.

Schluckner C., Subotić V., Lawlor V., Hochenauer C., 2014. Three-dimensional numerical and experimental investigation of an industrial-sized SOFC fueled by diesel reformat – Part I: Creation of a base model for further carbon deposition modeling. *Int. J. Hydrogen Energy*, 39, 19102–19118. DOI: 10.1016/j.ijhydene.2014.09.108.

Shen S., Ni M., 2015. 2D segment model for a solid oxide fuel cell with a mixed ionic and electronic conductor as electrolyte. *Int. J. Hydrogen Energy*, 40, 5160–5168. DOI: 10.1016/j.ijhydene.2015.02.074.

Sieniutycz S., Jeżowski J., 2009. *Energy optimization in process systems*. Ltd., Oxford.

Singhal S.C., 2000. Advances in solid oxide fuel cell technology. *Solid State Ionics*, 135, 305–313. DOI: 10.1016/S0167-2738(00)00452-5.

Singhal S.C., Kendall K., 2004. *High-temperature Solid Oxide Fuel Cells: Fundamentals, design and applications*. Elsevier, Oxford.

Stambouli A.B., Traversa E., 2002. Solid oxide fuel cells (SOFCs): A review of an environmentally clean and efficient source of energy. *Renewable Sustainable Energy Rev.*, 6, 433–455. DOI: 10.1016/S1364-0321(02)00014-X.

Vakouftsi E., Marnellos G.E., Athanasiou C., Coutelieris F., 2011. CFD modeling of a biogas fuelled SOFC. *Solid State Ionics*, 192, 458–463. DOI:10.1016/j.ssi.2010.05.051.

Zhang Z., Yue D., Yang G., Chen J., Zheng Y., Miao H., Wang W., Yuan J., Huang N., 2015. Three-dimensional CFD modeling of transport phenomena in multi-channel anode-supported planar SOFCs. *Int. J. Heat Mass Transfer*, 84, 942–954. DOI: 10.1016/j.ijheatmasstransfer.2015.01.097.

Ziółkowski P., Lemański M., Badur J., Nastałek L., 2012. Power augmentation of PGE Gorzow's gas turbine by steam injection – thermodynamic overview. *Rynek Energii*, 98, 161–167.

Ziółkowski P., Badur J., 2014. Navier number and transition to turbulence. *J. Phys. Conf. Ser.*, 530, 012035. DOI: 10.1088/1742-6596/530/1/012035.

Ziółkowski P. Kowalczyk T., Kornet S., Badur J., 2017. On low-grade waste heat utilization from a supercritical steam power plant using an ORC-bottoming cycle coupled with two sources of heat. *Energy Convers. Manage.*, 146, 158–173. DOI: 10.1016/j.enconman.2017.05.028.

Received 10 October 2017
Received in revised form 12 February 2018
Accepted 19 February 2018